AIN SHAMS UNIVERSITY
FACULTY OF ENGINEERING

Vol. 40, No. 4, December 31, 2005

SCIENTIFIC BULLETIN
Received on : 20/12/2005
Accepted on : 3/1/2006
pp. : 87-99

STRUCTURAL BEHAVIOR OF CONCRETE ENCASED STEEL BEAMS

Osama O. EL-MAHDY[1]

ABSTRACT

Concrete encased steel beams have been used extensively in bridges and buildings construction for many years. Investigations showed that such composite beams lead to a reduction of both structure weight and the resulted deformations. In the present paper, an accurate modeling for concrete encased steel beams is achieved by using the nonlinear three-dimensional finite element method through the general purpose computer program DIANA. The analysis takes into consideration the interaction between the steel and concrete to simulate the behavior of the encased beams well. The analysis has been performed for both linear and nonlinear stages. The results obtained from the present work are compared with the corresponding ones of previous available experimental works. The comparison showed that the present model is capable of introducing a good representation for the concrete encased steel beams behavior and strength.

KEYWORDS: Steel beams; Concrete; Composite beams; Interface bond; Nonlinear modeling; Finite element method.

الملخص العربي

في السنوات الأخيرة لوحظ زيادة استخدام الكمرات المركبة والتي تتكون من كمرة خرسانية تحتوي بداخلها على كمرة معدنية وقد تم استخدام هذا النوع من الكمرات فى منشآت المباني والكباري نظرا لما تتميز به من خواص انشائية عالية تجمع بين مميزات كلا من الحديد والخرسانة معا، وفى هذا البحث تم اقتراح نموذج لتحليل هذا النوع من الكمرات المركبة ، وقد تم استخدام طريقة العناصر المحددة والتحليل اللاخطى لنموذج مكون من الحديد والخرسانة يمثل الكمرة المركبة ، وقد تم تمثيل كلا من الحديد والخرسانة سواء في الضغط أو الشد بشكل دقيق وأيضا تم استخدام عناصر الاتصاق لتمثيل سطح التماس بين الحديد والخرسانة وقد تم دراسة نتائج الدراسة التحليلية من حيث الاجهادات الرئيسية وشكل التشكلات ووقيم المقاومة القصوى، وتم مقارنة هذه القيم بنتائج الدراسات المعملية المتاحة بواسطة باحثون آخرون ومن هذه المقارنة تم استنتاج أن النموذج المقترح يمثل هذه الكمرة بدقة تامة وبالتالي يمكن الاعتماد على النموذج التحليلي اللاخطى فى تحديد سلوك هذه الكمرات.

INTRODUCTION

The combination of steel and reinforced concrete, thereby utilizing the unique characteristics of the two materials, generally results in structures of greater

[1] Associate Professor, Faculty of Engineering at Shoubra, The University of Banha, EGYPT.

economy and safety than either material alone could achieve. Because of this, engineers have been continually interested in finding practical and effective ways of joining the materials, in developing new design concepts, and in establishing requirements for satisfactory performance. In the recent years, very significant advances have been made in all these areas, thus leading to a widespread use of combined steel and concrete elements in construction of buildings, bridges, nuclear power plants, and other types of engineering structures.

Basically, there are two ways that steel and concrete or elements made of them can be effectively combined. The first is to combine steel shapes with concrete to form individual members which can then be joined to make up a complete structure. The individual members or structures thus produced are called composite structures; typically examples are composite beams and floor slabs, steel reinforced concrete (SRC) beams or columns, concrete filled tubular columns, and steel section with partial concrete encasement. The second way is to develop efficient structural systems by combining steel frames with reinforced concrete elements, such as shear walls, and interior or exterior cores. These systems are called mixed or hybrid structural systems. Extensive research has been carried in many countries to study the behavior of composite and mixed structures and to develop criteria for the design (Metwally et al. 2000) and (Noguchi and Uchida 2004).

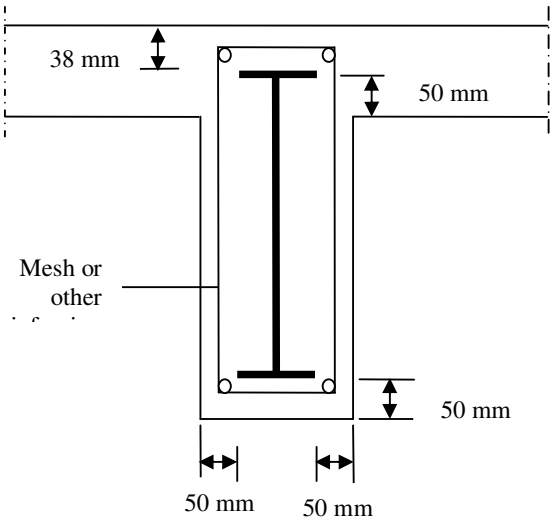

Fig.1. Encased Beam Minimum Cover Requirements

In this study, concrete encased steel beam shown in Fig. 1 is considered. These types of beams are widely used in buildings where the steel beams can be either totally or partial encased in concrete for fire protection. The fire resistance is due

to the fact that the concrete part prevents the inner steel parts - structural steel as well as reinforcing bars- from heating up too fast. In addition to the encased fire resistance, crippling and local buckling of the steel web is prevented and the resistance of the steel beam against lateral-torsional buckling is significantly increased. These beams also have greater stiffness under bending and vertical shear which results in a reduction of final deflection. Under some circumstances these encased beams can be designed using two alternatives as per ECP'01: a) The composite section properties shall be used in calculating bending stresses, neglecting concrete in tension and b) The steel beam alone is proportioned to resist all loads, live and dead, neglecting the composite action. No shear connectors, in the usual sense, are considered in this type of composite beam. The horizontal shear is transmitted from steel beam to concrete by friction and bond. In order to qualify as a composite beam, the concrete encasement must have mesh reinforcement throughout the whole depth and across the soffit of the steel beam, to prevent spalling of the concrete. The concrete encasement must also meet the minimum cover requirements according to LRFD Specifications' 1999 (refer to Fig. 1). The slab and the encasement must be cast integrally.

In actual practice, zero composite or non-integral action is impossible because there is always some degree of natural bond caused by chemical adhesion and mechanical friction between the concrete and steel beam. Similarly, 100 % or fully-integral composite action is impossible because there is always some small degree of slip. There are advantages to the encased beam which are usually overlooked. Only the compression area of the concrete is considered in the design. However, all of the concrete contributes a valuable reserve of shear strength to the beam. Also, the shrewd designer will utilize the additional stiffness of the encased beam when analyzing the building for combinations of vertical and lateral loads.

The main purpose of the present study is to summarize the results of the analysis that have been conducted to investigate the structural behavior of concrete encased steel beams using DIANA (Version 7) a general purpose finite element program. The nonlinear behavior of concrete in compression and tension, progressive cracking, and the bond-slip between steel and concrete are incorporated in the model. Predefined subroutines for material properties are coded. The validity of the model is studied by comparing analytical and experimental results which show an excellent agreement.

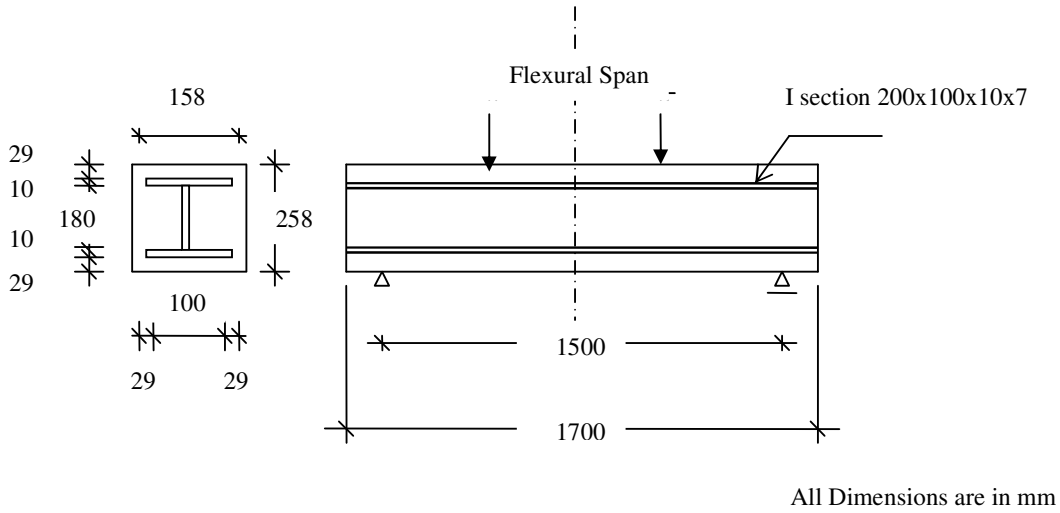

Fig. 2. Steel-Concrete Beam Reference Specimen

REFERENCE SPECIMEN AND FINITE ELEMENT MODELING

A three-dimensional finite element model of concrete encased steel beam shown in Fig. 2 is presented. This beam is selected for the analysis. It was experimentally tested by Miura et al. (1984). The symmetrical arrangement of the specimen made it possible to select only one-fourth of the concrete encased steel beam to be considered in the analysis. Appropriate boundary conditions are imposed on the symmetrical planes of the model. Figures 3 and 4 illustrate the finite element meshing that used in the analysis. Eight-node brick elements having three degrees of freedom at each node (HX24L in DIANA) are used to model both the concrete and steel parts. The concrete-steel behavior at the interfaces is idealized by using nodal and surface contact elements (N6IF and Q24IF in DIANA). The nodes of the finite element mesh are doubled at the steel-concrete interface for taking into consideration the bond. Frictional forces at the interface are neglected. The loads are applied to the specimen in the analysis. The model has 612 elements and 882 nodal points.

NONLINEAR MATERIAL MODELS

Modeling of Concrete

In tension, the concrete material is idealized as a linearly brittle material, assuming that cracks occur when the principal tensile stress exceeds the tensile strength. The concrete model is a smeared crack model in the sense that it does not track individual macro cracks. Bearing in mind that cracks may be closed and reopened again, a cracked element is checked in every iteration step for closure and reopening; a crack is closed or opened up if the stress normal to the crack surface is compressive or tensile, respectively.

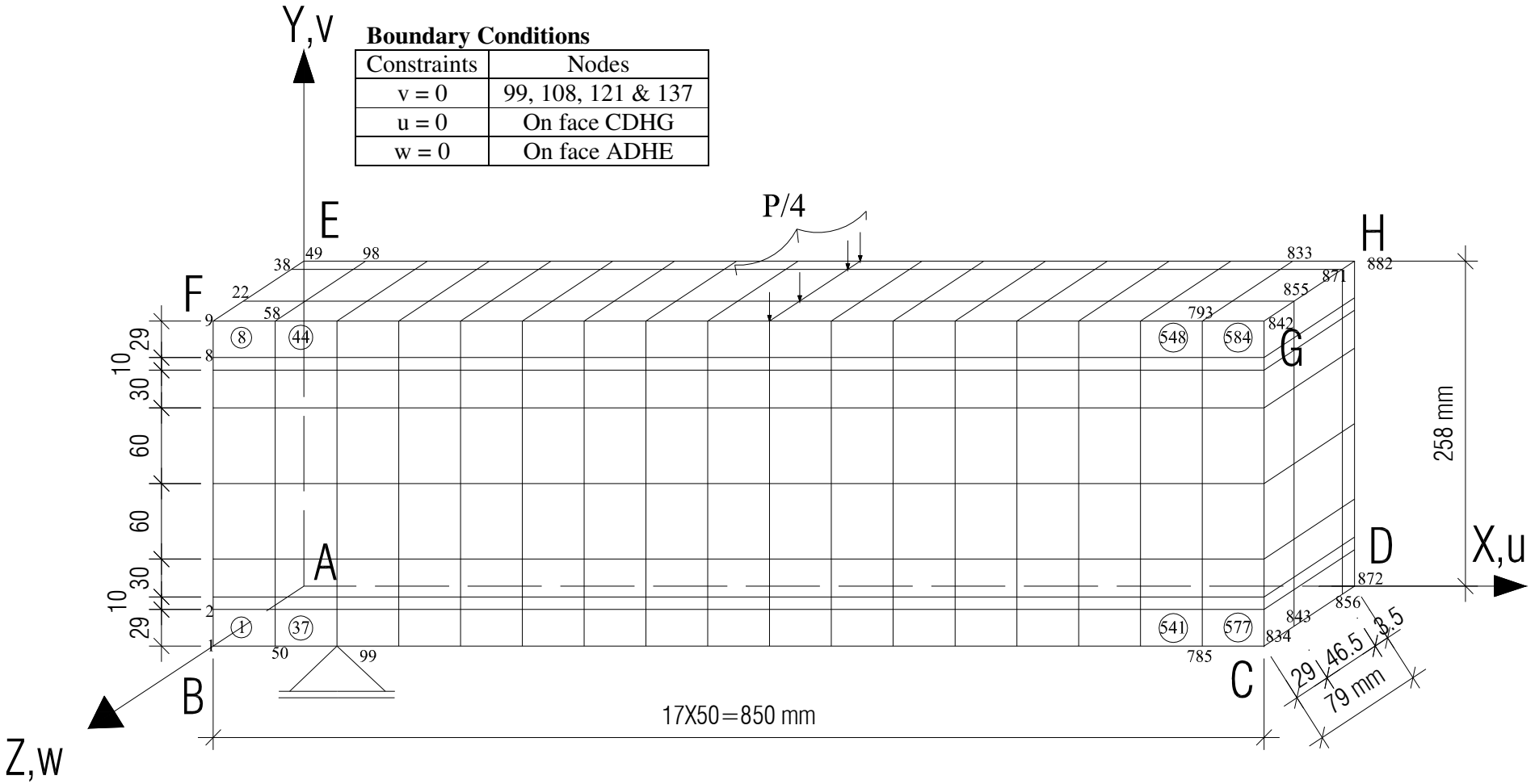

Fig. 3. Finite Element Meshing for One-Fourth of the Concrete Encased Steel Beam

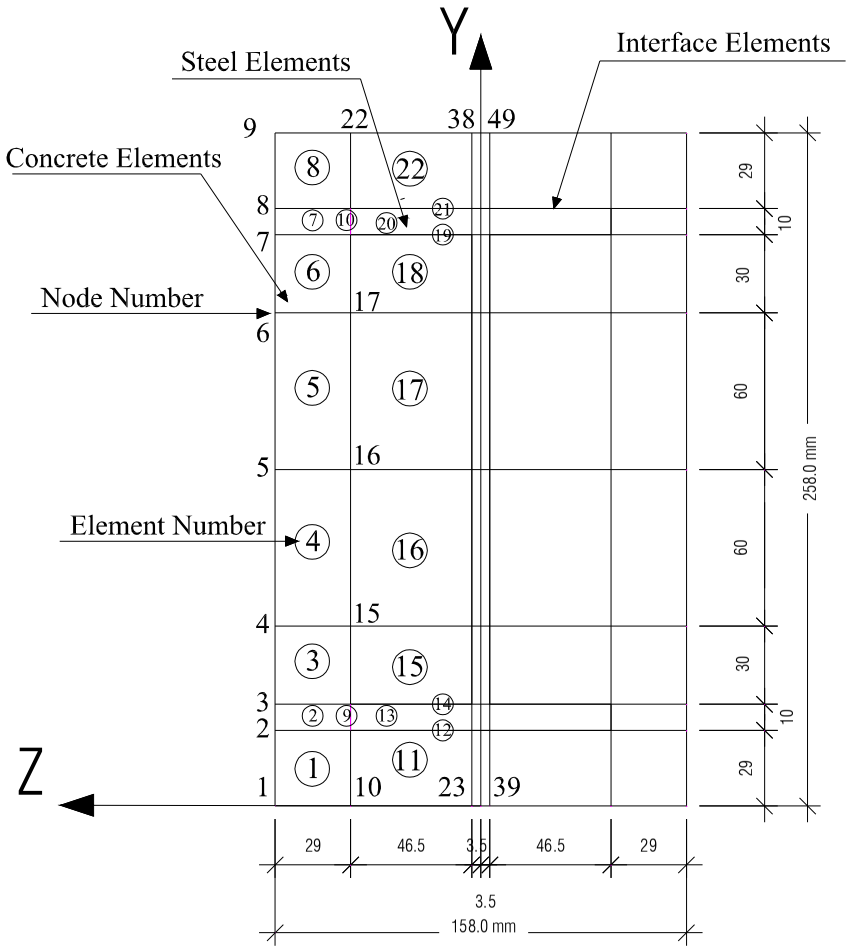

Fig. 4. Cross-Section Showing Interface Elements and the Double Noding

Before cracking, the material is assumed to be isotropic. After cracking, due to the presence of the crack surface, the material becomes anisotropic. For a cracked element, The Young's modulus normal to the crack surface and the shear modulus parallel to the crack surface are taken as zero. When a crack is closed, the Young's modulus normal to the crack surface is restored to the uncracked value and shear stress of the crack surface is assumed to be taken up by friction in a way similar to the interface elements. In addition, Poisson's effect can be considered negligible after cracking (Vecchio and Selby 1991).

In compression, the concrete material exhibits extensive nonlinearity in the stress-strain relation. As the solid elements are characterized by three-dimensional stress situation, the concrete material is under triaxial stresses. However, the triaxial stress state is approximately uniaxial (i.e. two of the principal stresses is much smaller than the third one). Therefore, the analysis can be simplified with the following assumptions: 1) The Young's modulus varies as a function of the larger compressive principal strain, as in the uniaxial case; 2) The Poisson's ratio remains constant at any stress level; and 3) The concrete is crushed when the principal compressive strain exceeds the ultimate limit and once the concrete fails in compression, it can never regain any strength.

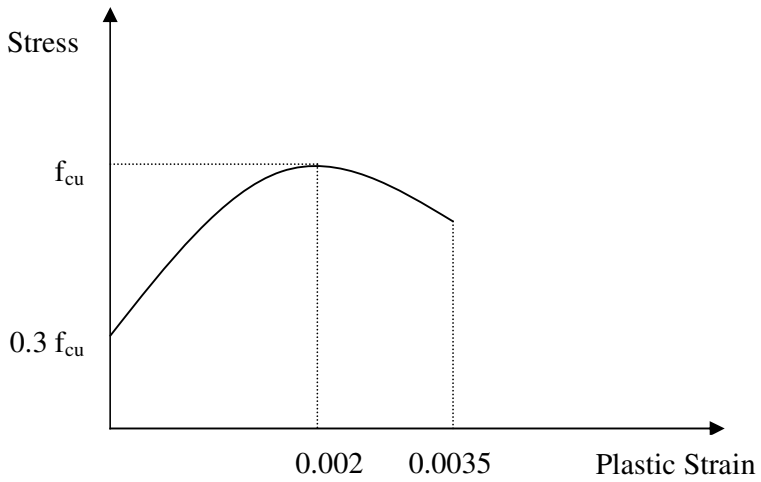

Fig.5. Stress-Plastic Strain Curve for Concrete under Uniaxial Compression

The concrete constitutive model in DIANA requires input of several parameters. These include points from the stress versus plastic strain curve in uniaxial compression, concrete uniaxial tensile strength, concrete biaxial compressive strength, principal component of plastic strain at ultimate state in biaxial compression and principal stress at cracking in plane stress when the other nonzero principal stress component is at its ultimate compressive stress value. The stress-plastic strain relationship for concrete under uniaxial compression is

shown in Fig. 5. DIANA default values are used for those parameter requiring biaxial test data. The concrete failure criteria follow Drucker-Prager in the space for principal stresses flow σ_1, σ_2, and σ_3, as shown in Fig. 6. The yield point has to be on the cone surface or inside it.

Modeling of Steel

The steel material is idealized as an isotropic elasto-plastic model based on the von Mises criterion.

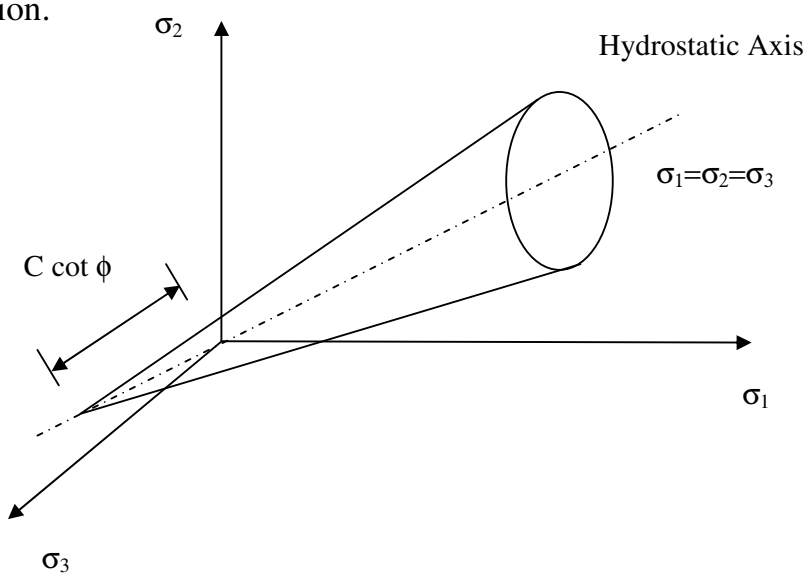

Fig. 6. Drucker-Prager Yield Criterion

Modeling of Bond

Plane linear quadrilateral and three dimensional nodal interface elements are utilized in the present analysis (refer to Fig. 3). These elements can be arranged along the entire steel-concrete interface and allow more rational use of load-slip relationships derived from previous experimental works (ASCE, 1982 and Plauk and Hees, 1981). The element constitutive relationship is formulated in terms of relative displacements of its top and bottom surfaces according to

$$F_s = K_s(\Delta_s - \Delta_r) \quad (1)$$

$$F_n = K_n \Delta_n \quad (2)$$

where F_s, F_n = Shear and normal forces at interface.

Δ_s , Δ_n = Relative slip and relative normal displacement of interface.

Δ_r , $\Delta_{r'}$ = Previous and new residual slips at interface.

K_s , K_n = Shear and normal stiffness of interface.

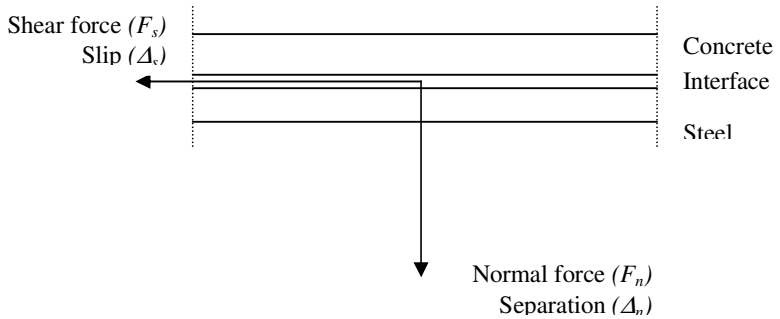

Fig. 7 Representation of Interface in Finite Element Analysis

Based on the experimental results for pull-out tests on flat plates with clear covers of 29 mm to the surface of the plate, a bilinear bond stress-slip relationship shown in Fig. 8 is used in the present analytical model. If the calculated friction is greater than the limiting friction, the friction developed is equated to the limiting friction and the residual slip Δ_r is reduced to

$$\Delta_{r'} = \Delta_s - (\frac{F_s}{K_s}) \tag{3}$$

As cracks develop and propagate, the interface normal and shear stiffness are changed. Furthermore, the interface elements are removed when the interface had separated.

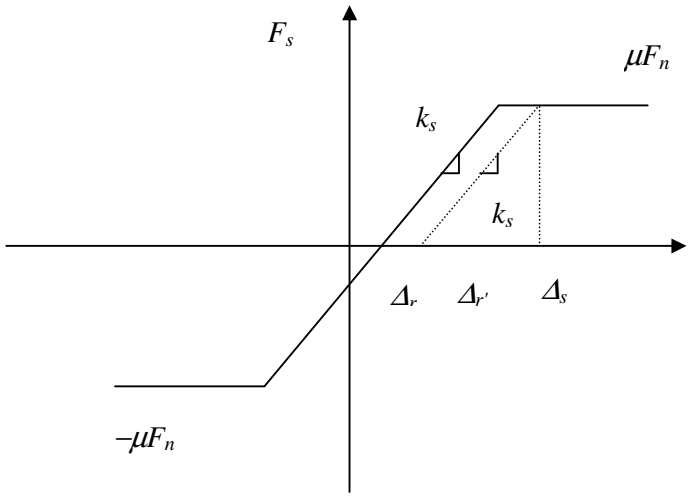

Fig. 8 Idealized Bond-Slip Relationship at the Interface

It may be assumed that complete interaction between steel and concrete is maintained under serviceability limit state. The complete interaction between steel and concrete shall be ensured in such a way that bond stresses between

steel and concrete shall not exceed 20 percent of bond strength under serviceability conditions (JSCE, 1986).

LOADING AND SOLUTION STRATEGY

Following the application the applied concentrated live load. A sufficient number of iterations are allowed during the analysis until a converged solution is reached. Convergence in DIANA is attained when the maximum residual nodal forces are less than a user-specified tolerance, which is defined as a small fraction of the applied nodal forces. The applied load is increased from zero to 10 KN in four steps. The load step size is then decreased to 1.50 KN up to a total load of 16 KN. Beyond this load and up to a load of 32 KN, a load step size of 1.0 KN is used. This is further reduced to 0.50 KN and the analysis is carried out up to a load of 52 KN. However, a singularity problem is encountered when the load is increased from 52 KN to 52.5 KN. The DIANA program indicated that the "plasticity algorithm did not converge at some node". The load step size is then decreased to 0.30 KN and the analysis is successfully performed to 56 KN. Once again, no converged solution is obtained between 56 KN and 56.30 KN. The solution is restarted from 56 KN using a load increment of 0.15 KN. However, the numerical problems are encountered as the load is increased to 64 KN. The load step size is decreased to 0.10 KN and the analysis is continued from a load of 64 KN. Converged solutions are reached as the load is increased beyond this pressure. Several unsuccessful attempts are made to continue the analysis beyond this load, but convergence could not be achieved.

ANALYTICAL RESULTS

Three analytical cases are investigated. In case 1, perfect bonding is assumed between the structural steel and the concrete beam. In case 2, zero bond is assumed between steel and concrete. In case 3, bond-slip model shown in Fig. 8 is utilized. The normal and shear stiffness of the plane and node interface elements are assumed to have either zero or infinite values in order to simulate the cases of no or perfect bond, respectively. Table (1) illustrates the obtained analytical results for the steel tensile stress and vertical displacement at the nodal point numbers 874 and 872, respectively (see Fig. 3).

Table 1. Tensile Stresses and Vertical Displacements Results

Case	Perfect Bond	Zero Bond	Bond-Slip
Steel Tensile Stress (N/mm^2)	340.48	425.60	383.04
Vertical Displacement (mm)	13.683	24.033	16.823

Ultimate Strength Results

The ultimate moment obtained using the present model is shown in Table 2. Furthermore, the comparison of the calculated value with those measured experimentally by Miura et al. 1984 is presented in this table. From this comparison, it can be concluded that the measured values are approximately greater than the calculated value only by about 7%.

Table 2. Results of the Obtained and Measured Ultimate Strength

Specimen No.	Measured Value M_{um} (KNm)	Calculated Value M_{uc} (KNm)	M_{um}/M_{uc}
1	79.990	73.26	1.09
2	78.284	73.26	1.07
3	76.224	73.26	1.04

Load-Deflection Relationship

Figure 9 shows the load-deflection curve at the nodal point of the mid-span obtained from the present analysis using bond-slip model. The degradation of the slope of this curve represents the effect of the reduced stiffness and the interface bond-slip. The analytical ultimate concentrated load is 256 KN.

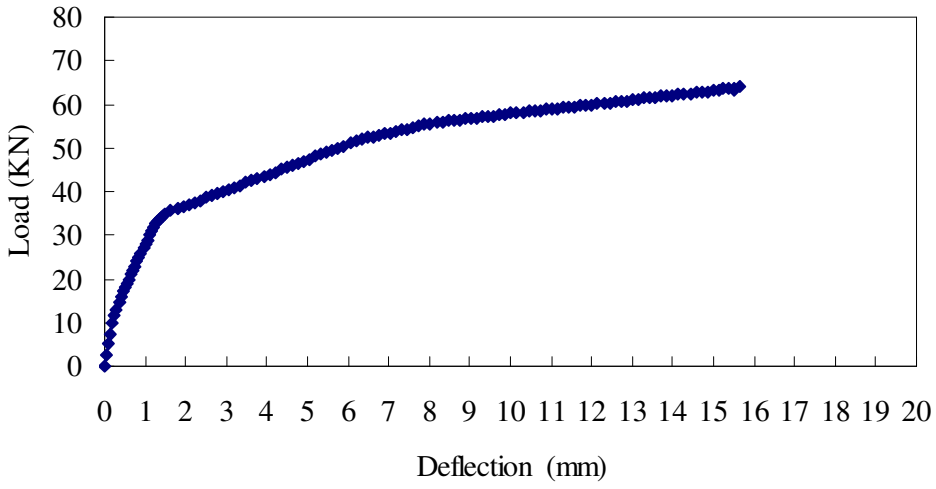

Fig. 9. Analytical Load-Deflection Curve

CONCLUSIONS

Although there are various types of composite structure, the common design method has not yet been established. Concrete encased steel beams are widely used in buildings. However, there have been few experimental or analytical studies on this area. The reluctance of practicing engineers to take the more accurate behavior of these beams has been, firstly, due to lack of knowledge concerning the composite behavior and secondly, due to lack of practical methods for predicting the stiffness and strength. This paper concerns the development of a three-dimensional nonlinear finite element model for studying the behavior of concrete encased steel beams beam specimen that was previously tested by Miura et al. with regards to both serviceability and ultimate limit states. The nonlinear behavior of component materials (concrete cracking, nonlinear behavior of concrete, yield of steel beam, and bond-slip relationship at the interface), is adequately considered in the model. The results obtained from this model are compared with the measured experimental ones. The comparison demonstrates that the proposed finite element model is accurate enough to model this type of composite beams. This model may therefore, serve as a simulation tool or as a means to improve design codes as well.

REFERENCES

1. Noguchi, H. and Uchida, K., (2004), "Finite Element Method Analysis of Hybrid Structural Frames with Reinforced Concrete Columns and Steel Beams", Proceedings of Journal of Structural Engineering, ASCE, Vol. 130, No. 2, pp. 328-335.
2. Metwally, M.E.A., Allam, H.M., and Atia, A.H., (2000), "Shear Behavior of Concrete Beams with Embedded Steel Sections", Proceedings of The Second International Conference on Civil Engineering, Faculty of Engineering, Helwan University, pp. 175-183.
3. ECP'01, (2001), "Egyptian Code of Practice for Steel Construction and Bridges", Ministerial Decree No. 279-2001.
4. LRFD Specification for Structural Steel Buildings, (1999), American Institute for Steel Construction, INC., Chicago, Illinois, 60601-2001.
5. DIANA 7 "Finite Element Analysis", TNO Buildings and Construction Research, Netherlands.
6. Vecchio, F.J. and Selby, R.G., (1991), "Toward Compression-Field Analysis of Reinforced Concrete Solids", Proceedings of Journal of Structural Engineering, ASCE, Vol. 117, No. 6, pp. 1740-1758.
7. ASCE Task Committee on Finite Element Analysis of Reinforced Concrete Structures, (1982), "State-of-the-Art Report on Finite Element Analysis of Reinforced Concrete", American Society of Civil Engineers, New York.

8. Plauk, G., and Hees, G., (1981), "Finite Element Analysis of Reinforced Concrete Beams with Special Regard to Bond Behavior", Proceedings of IABSE Colloquium on "Advanced Mechanics of Reinforced Concrete", Vol. 34, pp. 655-670.
9. Standard Specifications for Design and Construction of Concrete Structures (1986) Part 1 (Design), Japan Society of Civil Engineers (JSCE), Tokyo, Japan.
10. Miura, T., Sano, M. and Sato, M., (1984), “Properties of Concrete Beams Reinforced with Deformed Steel Bars, Plates or Shapes”, Transactions of The Japan Concrete Institute, Vol. 6, pp. 449-456.